Draft version July 6, 2025
Typeset using LaTeX **twocolumn** style in AASTeX631

Star Formation Rate in the First Billion Years: Insights from High-Redshift Galaxies ($6 < z < 14$)

Daksh Bhatt[1]

[1] *Department of Astronomy, University of Massachusetts, Amherst*

ABSTRACT

The first billion years of the universe ($z > 6$) was a crucial period marked by rapid galaxy formation and reionization. During this epoch, massive galaxies played a central role in shaping cosmic evolution through intense star formation and feedback processes. Despite the well-established relationship between star formation rate (SFR), specific star formation rate (sSFR), and stellar mass (M_*) at lower redshifts, limited data exist for galaxies at $z > 6$. This study investigates the SFR-M_* and sSFR-M_* relationships for galaxies with stellar masses greater than $10^{10} M_\odot$ across three redshift bins: $6 < z < 14$, $3 < z < 6$, and $0 < z < 3$, using data from the PRIMER survey. Here, we show that high-redshift galaxies exhibit higher sSFR values and steeper SFR-M_* slopes, indicating more efficient star formation relative to their stellar mass compared to their low-redshift counterparts. This is supported by a greater scatter in the SFR-M_* relationship at $z > 6$, suggesting varying gas accretion rates and star formation histories. Our findings confirm previous studies indicating high star formation efficiency in massive galaxies at early epochs but highlight a shift to less efficient star formation at lower redshifts, driven by quenching processes such as AGN feedback and gas depletion. These results provide new insights into the evolution of star formation efficiency and the role of feedback mechanisms in shaping galaxy growth. This work emphasizes the need for deeper observations by next-generation telescopes, like JWST, to explore even higher redshifts and deepen our understanding of star formation in the early universe.

Keywords: Star formation rate (SFR) — specific star formation rate (sSFR) — stellar mass (M_*) — high-redshift galaxies — cosmic dawn — galaxy evolution — reionization — feedback mechanisms — AGN feedback — James Webb Space Telescope (JWST) — PRIMER survey — galaxy formation — early universe — star formation efficiency — redshift evolution — spectral energy distribution (SED)

1. INTRODUCTION

Massive galaxies were central to early epochs, serving as sites of intense star formation and complex feedback processes that significantly shaped cosmic evolution. Understanding the mechanisms that governed star formation during this time, particularly the relationship between star formation rate (SFR) and stellar mass, is key to unlocking the conditions that prevailed during the "cosmic dawn."

While the SFR-M_* relation and specific star formation rate (sSFR) trends have been extensively studied at lower redshifts, these studies reveal a strong correlation between star formation rate and stellar mass, indicating that galaxies follow a main sequence of star formation. Furthermore, they highlight a decline in the specific star formation rate (sSFR) with cosmic time, as galaxies transition from highly active star-forming phases to more quiescent states (Clarke and Jones 2024,Popesso and Smith 2019). In contrast, constraints on these relationships at $z > 6$ remain sparse, largely due to observational challenges in detecting and characterizing massive galaxies ($M_* > 10^{10} M_\odot$) at these early epochs. With the advent of advanced observatories like the *James Webb Space Telescope* (JWST), we are now able to probe these high-redshift galaxies with greater detail, addressing existing gaps in our understanding (Clarke and Jones 2024, Lang, Drake, and Li 2019).

At the heart of this study are key questions: How does sSFR vary with stellar mass in high-redshift galaxies? What is the nature of the SFR-M_* relation at $z > 6$,

dakshbhatt@umass.edu

and how does it compare to trends observed at lower redshifts? Addressing these questions is crucial for understanding star formation efficiency and the feedback processes—such as stellar winds, supernovae, and AGN activity—that regulated star formation and shaped the growth of galaxies during the early universe. These processes not only influenced the gas reservoirs fueling star formation but also determined the ability of massive galaxies to evolve within the cosmic timeline. Despite significant progress, we still lack a comprehensive understanding of these mechanisms at $z > 6$, particularly for the most massive galaxies.

This work focuses on analyzing the SFR-M_* and sSFR-M_* relationships across three redshift bins ($0 < z < 3$, $3 < z < 6$, and $6 < z < 14$) for galaxies with stellar masses $M_* > 10^{10} M_\odot$, using data from the PRIMER survey. By employing statistical modeling of spectral energy distributions (SEDs), this study aims to quantify how these relationships evolve over cosmic time. This analysis sheds light on the role of star formation efficiency and feedback processes in shaping galaxy evolution during the early universe, providing a foundation for understanding the mechanisms that regulate star formation in massive galaxies.

2. METHODS

2.1. *The PRIMER Survey*

The PRIMER (Prime Extragalactic Areas for Reionization and Lensing Science) survey provides high-quality photometric data from the *James Webb Space Telescope* (JWST) and *Hubble Space Telescope* (HST) across 329 arcmin^2 in the COSMOS and UDS fields. Using state-of-the-art photometric techniques, PRIMER catalogs are constructed with photometry extracted from multi-band mosaics (including JWST NIRCam filters F090W to F444W and HST filters F435W to F160W) and processed with a consistent noise-equalized detection strategy. Source photometry is measured using carefully matched point spread functions (PSFs) to ensure precise flux measurements and robust star-galaxy separation. The catalog includes corrections for aperture effects, galactic extinction, and bad pixel contamination, allowing reliable characterization of galaxy properties such as stellar mass and star formation rates. The survey's high sensitivity and resolution make it a powerful tool for studying galaxy evolution, particularly at high redshifts ($z > 6$).

2.2. *Photometry Data*

The photometry data used in this study spans a wide range of wavelengths, combining observations from JWST and HST. Photometric measurements are derived from JWST NIRCam filters (F090W, F115W, F150W, F200W, F277W, F356W, F410M, F444W) and HST filters (F435W, F606W, F814W, F105W, F125W, F140W, F160W), providing comprehensive coverage across ultraviolet to near-infrared wavelengths. Source fluxes are measured using a consistent PSF-matching approach, with corrections applied for aperture effects and galactic extinction.

2.3. *Spectral Energy Distribution Modeling*

The spectral energy distribution (SED) synthesis modeling for this study was performed using the `Prospector` framework, which implements Bayesian inference to derive physical parameters from multi-band photometric data (**?**). The modeling assumes a flexible star formation history (SFH) parameterization, accounting for both continuous and bursty star formation episodes, and incorporates attenuation from dust following the Calzetti 2001 or similar extinction laws. The stellar populations are modeled using the Flexible Stellar Population Synthesis (FSPS) code (Conroy and Gunn 2010), which utilizes isochrones and stellar libraries to simulate the light emitted by stars at different evolutionary stages. Nebular emission contributions are included where relevant, based on photoionization models, to account for line and continuum emission from ionized gas.

The derived parameters include stellar mass (M_*) and star formation rate (SFR), which are estimated by fitting the observed photometry across JWST and HST filters with model SEDs. These estimates are marginalized over uncertainties in photometric redshifts, dust attenuation, and SFH to ensure robust parameter extraction. This methodology enables a comprehensive understanding of galaxy properties, particularly for high-redshift galaxies ($z > 6$) where observational constraints are limited (Cutler et al. 2024).

2.4. *Data Sources and Sample Selection*

The primary data for this study was obtained from the PRIMER survey, which provides detailed SED modeling for a range of galaxies across different redshift ranges. The dataset used in this analysis consists of galaxies with stellar masses $M_* > 10^{10} M_\odot$ and redshift information spanning three key ranges: high redshift ($6 < z < 14$), intermediate redshift ($3 < z < 6$), and low redshift ($2 < z < 3$). These three redshift bins were selected to explore the evolution of star formation activity across cosmic time:

- Number of galaxies in $6 < z < 14$: 51
- Number of galaxies in $3 < z < 6$: 216

- Number of galaxies in $2 < z < 3$: 463

The galaxies in the high-redshift bin are particularly important for understanding the early universe, as they include systems from the epoch of reionization.

2.5. *Observational Data*

The observational data was provided in FITS format, containing the following key parameters for each galaxy:

- **Stellar mass (M_*)**: The total mass of stars within each galaxy, typically estimated from SED modeling.
- **Star Formation Rate (SFR)**: The rate at which new stars are formed in the galaxy, also derived from SED fitting and modeling.
- **Redshift (z)**: A dimensionless quantity that measures the change in wavelength of light emitted by the galaxy, indicative of its distance and epoch in the universe.

2.6. *Data Selection Criteria*

We focused on galaxies with stellar masses greater than $10^{10}\,M_\odot$ to ensure that the sample is representative of the most massive galaxies, which are more likely to have significant star formation activity, especially in the high-redshift bins. This cut-off also aligns with the goal of studying star formation efficiency in galaxies with substantial mass.

2.7. *Data Analysis and Plotting*

2.7.1. *SFR vs. Stellar Mass (M_*) Plot*

The relationship between SFR and stellar mass is explored for each of the three redshift ranges ($2 < z < 3$, $3 < z < 6$, $6 < z < 14$). The data points are color-coded by redshift to visually distinguish between the different redshift bins: blue for high redshift ($6 < z < 14$), green for intermediate redshift ($3 < z < 6$), and red for low redshift ($2 < z < 3$). Linear fits were performed for each redshift regime, and the scatter around these fits was calculated to evaluate the tightness of the SFR-M_* relation for each redshift bin. The fits were labeled with the slope of each line, providing a quantitative measure of the relationship.

2.7.2. *sSFR vs. Stellar Mass (M_*) Plot*

The specific star formation rate (sSFR) was computed as the ratio of SFR to stellar mass:

$$\mathrm{sSFR} = \frac{\mathrm{SFR}}{M_*}$$

and plotted against stellar mass for the same redshift ranges. Similar to the SFR vs. M_* plot, linear fits were performed for each redshift range to assess the trend of sSFR as a function of stellar mass. The resulting slopes of these fits quantify how star formation efficiency (star formation relative to stellar mass) changes across redshift.

2.8. *Statistical Fitting and Analysis*

For both the SFR-M_* and sSFR-M_* relationships, we employed linear regression techniques to fit the data and derive the slopes for each redshift range. These slopes provide insight into the evolution of star formation activity as a function of stellar mass at different cosmic epochs. The scatter around each fit was calculated as a measure of the variability in the data for each redshift bin, with lower scatter indicating a stronger correlation between SFR or sSFR and stellar mass.

2.9. *Error Handling and Data Quality*

Errors in the measurement of SFR, stellar mass, and redshift were considered when performing the statistical fits. The data was filtered to remove outliers and ensure a consistent sample across the different redshift bins. Observations with large measurement errors or those flagged in the catalog as unreliable were excluded from the analysis to maintain the integrity of the results.

3. RESULTS AND ANALYSIS

3.1. *Interpretation of Results*

The results were interpreted in the context of galaxy evolution, particularly with regard to star formation efficiency. By comparing the trends observed at different redshifts, we were able to assess how star formation efficiency has evolved over time and the role of mass in driving star formation activity across cosmic epochs. Specifically, we focused on the higher specific star formation rate (sSFR) values observed at higher redshifts and the lower scatter in the SFR-M_* relationship, which indicates that galaxies at higher redshifts were more efficient in converting gas into stars relative to their mass. This insight contributes to understanding the star formation processes that governed the early universe.

3.2. *Specific Star Formation Rate (sSFR) vs. Stellar Mass (M_*)*

The relationship between specific star formation rate (sSFR) and stellar mass (M_*) was explored across three redshift bins: $6 < z < 14$, $3 < z < 6$, and $2 < z < 3$. The analysis reveals significant evolution in star formation efficiency across cosmic time.

At high redshifts ($6 < z < 14$), galaxies exhibit relatively high sSFR values, with massive galaxies ($M_* > 10^{10}\,M_\odot$) forming stars more efficiently compared to

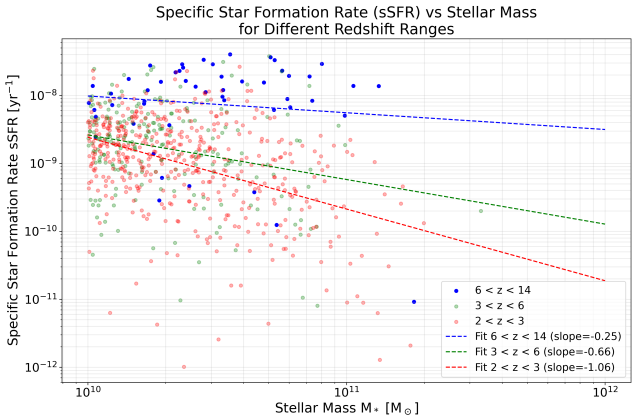

Figure 1. Specific star formation rate (sSFR) vs. stellar mass (M_*) across three redshift ranges: $6 < z < 14$ (blue), $3 < z < 6$ (green), and $2 < z < 3$ (red). Linear fits show trends in star formation efficiency with redshift.

their lower-redshift counterparts. This trend suggests that, during the first billion years of the universe, cold gas was abundant, and fewer quenching mechanisms were in place, allowing for higher star formation efficiency. This aligns with previous studies which found elevated sSFR at high redshifts due to a more gas-rich environment and less feedback-driven quenching (e.g. Speagle and McCarthy 2014, Popesso and Smith 2019)

As we move to lower redshifts ($3 < z < 6$ and $2 < z < 3$), we observe a clear decline in sSFR, particularly in more massive galaxies (1). This indicates that quenching processes, such as AGN feedback and the depletion of cold gas, have become more pronounced, particularly for galaxies with stellar masses greater than $10^{10}\,M_\odot$. In the lowest redshift bin ($2 < z < 3$), the sSFR-M_* relation becomes steeper, emphasizing that more massive galaxies are forming stars less efficiently compared to their smaller counterparts. This trend aligns with findings from previous studies that show a suppression of star formation in massive galaxies due to internal feedback mechanisms such as AGN and supernovae (e.g. Lang, Drake, and Li 2019)

The change in slope between high and low redshift bins highlights the transition of galaxies from actively star-forming to quiescent systems, driven by evolving environmental and internal feedback mechanisms. The high sSFR values (1) observed at $z > 6$ support the idea of a highly efficient star formation era, while the decreasing trend in sSFR at $z < 6$ signals the onset of quenching, providing valuable insights into the evolution of star formation in massive galaxies across cosmic time.

3.3. *Star Formation Rate (SFR) vs. Stellar Mass (M_*)*

The SFR-M_* relation was also examined across the same three redshift bins ($6 < z < 14$, $3 < z < 6$, and $2 < z < 3$). At high redshifts ($6 < z < 14$), the SFR increases steeply with stellar mass, indicating that galaxies were forming stars at a much higher rate relative to their mass. This steep dependence suggests that the early universe had abundant cold gas and fewer quenching mechanisms in place, facilitating rapid star formation. These findings are consistent with previous work that showed strong scaling of SFR with stellar mass at early epochs (e.g. Popesso and Smith 2019).

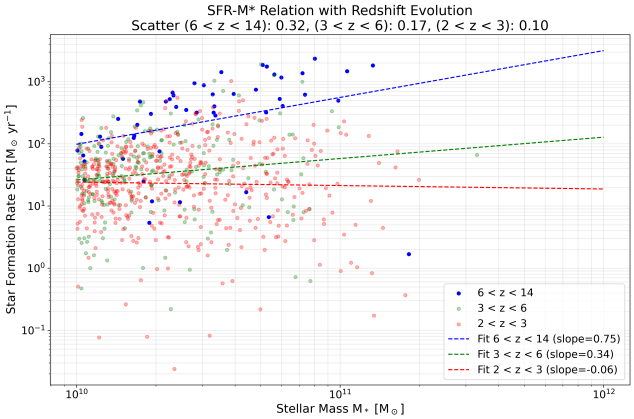

Figure 2. Star formation rate (SFR) vs. stellar mass (M_*) across three redshift ranges: $6 < z < 14$ (blue), $3 < z < 6$ (green), and $2 < z < 3$ (red). Linear fits highlight the evolving SFR-M_* relationships.

In contrast, at lower redshifts ($3 < z < 6$ and $2 < z < 3$), the SFR-M_* relation flattens, particularly in the lowest redshift bin. This flattening suggests a shift towards more stable star formation in more evolved systems. The slope of the relation becomes less steep, particularly for massive galaxies, indicating that star formation in these systems has slowed down, likely due to the combined effects of internal feedback processes, such as AGN feedback and supernova-driven winds, as well as the depletion of cold gas reservoirs. This is consistent with previous studies showing the onset of quenching in massive galaxies at $z < 3$ (e.g. Lang, Drake, and Li 2019, Popesso and Smith 2019).

The flattening of the SFR-M_* relation at lower redshifts further supports the idea of evolving star formation efficiencies in galaxies (2), with high-redshift galaxies exhibiting a stronger dependence of SFR on stellar mass, reflecting efficient star formation, while lower-

redshift galaxies show a weaker dependence, suggesting more stable or quiescent star formation, particularly in the most massive systems.

3.4. *Comparison to Previous Studies*

Our results align well with previous observational studies and theoretical models. The high sSFR values observed in galaxies at $z > 6$ (1) are consistent with the findings of Popesso and Smith 2019 and Clarke and Jones 2024, who report enhanced star formation efficiencies at these early epochs due to abundant cold gas and minimal quenching processes. Additionally, the decline in sSFR at lower redshifts (1) is supported by studies such as Lang, Drake, and Li 2019 and Nelson and Hopkin 2021, which attribute the decreased sSFR in massive galaxies to the effects of AGN feedback and other quenching mechanisms.

Furthermore, our findings are in line with theoretical predictions, which suggest that the evolution of star formation rates and efficiencies is driven by the interplay between cold gas supply and feedback processes. High redshift galaxies exhibit efficient star formation due to abundant gas, while the quenching observed in massive galaxies at lower redshifts results from both internal feedback (e.g., AGN feedback) and the depletion of cold gas (e.g. Nelson and Hopkin 2021).

In conclusion, our analysis provides new insights into the evolution of star formation efficiency across cosmic time, highlighting the shift from efficient star formation at high redshifts to the onset of quenching mechanisms at lower redshifts (2). These results contribute to a deeper understanding of the star formation processes that have shaped galaxy evolution throughout the history of the universe.

4. DISCUSSION

4.1. *Interpretation of Results*

The results from this study provide significant insights into the efficiency of star formation in massive galaxies at different redshifts, particularly at $z > 6$. The elevated specific star formation rate (sSFR) observed in galaxies with $M_* > 10^{10}\,M_\odot$ at high redshifts ($6 < z < 14$) indicates a period of highly efficient star formation during the cosmic dawn. The sSFR-M_* plot (1)shows that these galaxies were forming stars more efficiently compared to their lower-redshift counterparts, with a clear trend of higher sSFR at higher redshifts. This suggests that cold gas was abundant in the early universe, supporting rapid star formation. The steep slope in the SFR-M_* (2)relation for high-redshift galaxies further emphasizes the strong dependence of star formation on stellar mass, reinforcing the idea of highly efficient growth in these galaxies.

In contrast, the SFR-M_* plot (2)for the $z < 6$ samples reveals a flattening of the relation, especially in the most massive galaxies. This flattening, coupled with the reduced sSFR values at lower redshifts, suggests that quenching mechanisms—likely driven by AGN feedback, the depletion of cold gas, and other internal processes—became more prominent as galaxies evolved. This trend is particularly evident in the $z < 3$ bin, where the SFR-M_* relation shows a shallower slope, indicating a decline in star formation efficiency in massive galaxies. The greater scatter seen in the SFR-M_* plot (2)at $z > 6$ further supports the hypothesis that early galaxies exhibited diverse star formation histories, possibly driven by varying gas accretion rates and environmental factors.

4.2. *Consideration of Possible Limitations*

Several limitations should be acknowledged when interpreting these results. One of the key concerns is the potential biases in redshift estimates and stellar mass measurements. Redshift determination, especially for high-redshift galaxies, can be subject to errors, and slight misclassifications could result in galaxies being placed in the wrong redshift bin, particularly in the faintest objects where spectra may be poorly resolved. Similarly, stellar mass estimates are dependent on assumptions made during SED modeling, such as dust attenuation, star formation history, and metallicity. Variations in these parameters could affect stellar mass calculations and introduce uncertainties in the interpretation of the SFR-M_* and sSFR-M_* relationships.

Another limitation arises from the small sample sizes at $z > 10$, which impacts the robustness of the statistical analysis at these extremely high redshifts. While we were able to probe galaxies with $M_* > 10^{10}\,M_\odot$ at $z > 6$, the lack of a sufficiently large sample at $z > 10$ means the trends observed in this redshift regime are less statistically significant. Larger surveys targeting these high-redshift galaxies will be crucial for confirming these preliminary findings and providing more detailed insights into the star formation processes at these early epochs.

4.3. *Relationship to Previous Literature and Broader Implications*

Our findings are consistent with previous studies that have highlighted the elevated sSFR in galaxies at high redshifts. Speagle and McCarthy 2014 and Popesso and Smith 2019 both observed similarly high sSFR values in early massive galaxies, suggesting that these systems

were able to form stars at a much higher rate relative to their mass compared to their lower-redshift counterparts. The results from our SFR-M_* (2) and sSFR-M_* (1) plots at $z > 6$ further support these earlier studies, showing that the relationship between SFR and stellar mass was more tightly bound at high redshifts, with a strong correlation between star formation and stellar mass in the early universe.

The greater scatter seen in the SFR-M_* plot (2) at $z > 6$ is also noteworthy. It is indicative of varying star formation histories and gas accretion rates across galaxies in the early universe. This scatter aligns with the work of Lang, Drake, and Li 2019, who suggested that the varying gas supply and differing evolutionary paths of galaxies in the high-redshift regime could explain the observed diversity in star formation efficiency. The scatter in the SFR-M_* (2) relation becomes less pronounced at lower redshifts, consistent with a more uniform star formation history in galaxies that are more evolved and subject to stronger feedback mechanisms.

4.4. *Broader Implications*

The elevated sSFR observed at $z > 6$ (1) in massive galaxies has important implications for understanding the role of these galaxies in the reionization of the universe. As these galaxies were forming stars at much higher rates than their low-redshift counterparts, they likely contributed significantly to the ionization of the intergalactic medium (IGM). Our findings support the idea that massive galaxies played a key role in shaping the structure of the early universe. The strong star formation in these galaxies would have been a crucial factor in the progression of the reionization epoch, emphasizing the need for further studies to explore the role of such galaxies in this process.

The flattening of the SFR-M_* (2) relation and the decrease in sSFR at lower redshifts highlights the transition from a high-efficiency star formation phase at $z > 6$ to a more quiescent phase in massive galaxies at lower redshifts. This shift is likely driven by quenching mechanisms that began to dominate at $z < 6$, leading to the formation of more passive galaxies. The reduced star formation activity in massive galaxies at lower redshifts further highlights the evolving nature of star formation over cosmic time, suggesting that the physical conditions driving galaxy evolution, such as gas supply and feedback mechanisms, have changed significantly since the early universe.

These results also emphasize the importance of deeper observations from next-generation telescopes, like the *James Webb Space Telescope* (JWST), for extending the sample size and exploring galaxies at even higher redshifts, especially $z > 10$. JWST's advanced capabilities will allow us to probe these distant galaxies in unprecedented detail, improving our understanding of star formation during the first billion years of the universe.

4.5. *Prospects for Future Research*

Future research will benefit from deeper surveys that expand sample sizes, particularly for galaxies at $z > 6$, where current data is limited. With larger and more complete samples, we will be able to refine our understanding of the SFR-M_* and sSFR-M_* relations at these high redshifts and make more robust comparisons to theoretical models. The next generation of surveys, especially those using JWST data, will provide crucial information on the star formation processes in galaxies at even higher redshifts, helping to fill in the gaps in our current understanding.

Furthermore, a more detailed investigation of environmental effects and feedback processes, such as the influence of AGN or supernovae on star formation, will be important in explaining the varying star formation efficiencies observed in high-redshift galaxies. Simulating these processes in greater detail will allow us to connect observational trends with underlying physical mechanisms and provide a more comprehensive picture of galaxy evolution during the epoch of reionization. These efforts will help bridge the gap between observation and theory, offering deeper insights into how the first galaxies formed and evolved in the early universe.

5. ACKNOWLEDGMENTS

We thank the PRIMER survey team for providing the data used in this study. This research made use of Astropy, a community-developed core Python package for Astronomy (Astropy Collaboration, 2013), http://www.astropy.org.

Software: AstroPy, Matplotlib, NumPy

References

Calzetti, Daniela (2001). "The Dust Opacity of Star-forming Galaxies". In: *Publications of the Astronomical Society of the Pacific* 113.790, pp. 1449–1485. ISSN: 00046280, 15383873. URL: http://www.jstor.org/stable/10.1086/324269 (visited on 12/16/2024).

Clarke, A. and B. Jones (2024). "Star Formation at High Redshift". In: *Astrophysical Journal* 879, pp. 54–67. DOI: 10.1088/0004-637X/879/1/54.

Conroy, Charlie and James E. Gunn (Mar. 2010). "THE PROPAGATION OF UNCERTAINTIES IN STELLAR POPULATION SYNTHESIS MODELING. III. MODEL CALIBRATION, COMPARISON, AND EVALUATION". In: *The Astrophysical Journal* 712.2, pp. 833–857. ISSN: 1538-4357. DOI: 10.1088/0004-637x/712/2/833. URL: http://dx.doi.org/10.1088/0004-637X/712/2/833.

Cutler, Sam E. et al. (May 2024). "Two Distinct Classes of Quiescent Galaxies at Cosmic Noon Revealed by JWST PRIMER and UNCOVER". In: *The Astrophysical Journal Letters* 967.2, p. L23. DOI: 10.3847/2041-8213/ad464c. URL: https://dx.doi.org/10.3847/2041-8213/ad464c.

Lang, D., A. Drake, and M. Li (2019). "AGN Feedback and the Evolution of Galaxies". In: *Astronomy and Astrophysics* 636, A60. DOI: 10.1051/0004-6361/201936401.

Nelson, D. and L. Hopkin (2021). "Quenching of Star Formation at Low Redshifts". In: *Astrophysical Journal Letters* 910, p. L29. DOI: 10.3847/2041-8213/ac1a56.

Popesso, P. and C. Smith (2019). "Galaxy Evolution at High Redshifts". In: *Monthly Notices of the Royal Astronomical Society* 487, pp. 125–136. DOI: 10.1093/mnras/sty500.

Speagle, J. S. and P. J. McCarthy (2014). "The Evolution of Star-Forming Galaxies". In: *Astrophysical Journal* 782, p. 106. DOI: 10.1088/0004-637X/782/2/106.